High-Resolution Small Diameter EMAT Crack ILI Tool for Difficult to Inspect Piping

Final Report

Deliverable

P. Bondurant
K. Hay
D. Westerling
Dr. H. Kannajosyula
Dr. G. Nino

June 15, 2020

Prepared for

Operations Technology Development (OTD)

LEGAL NOTICE

PORTIONS OF THIS REPORT ARE PATENT PENDING

Quest Integrated, LLC
19823 58th Place S, Suite 200
Kent, Washington 98032
(253) 872-9500

1. SUMMARY

The project objective is to build and test an Electro-Magnetic Acoustic Transducer (EMAT) tool prototype to detect and quantify longitudinal cracks in metallic pipes. The sensor will be used to assess small-diameter and unpiggable pipes containing fittings and other restricting features. A previous Gas Technology Institute contract (S594), referred to as Phase 2 in the report, resulted in a tethered tool connected via Ethernet to an external computer for data analysis. Laboratory work demonstrated that all the defects in the test samples were detectable by the tool as well as blind defects during demonstrations at Quanta Inline Devices (Q-Inline) in Texas and the PGE facility in California. Therefore, the purpose of EMAT/CRACK Phase 3, this project, was the development of a fieldable EMAT-based unpressurized wireline tool system with a maximum speed of 0.5 m/s to detect cracks on 8" diameter pipes.

With the aim to achieve the project goals, this program was divided in five main activities: (i) System design that includes electrical and mechanical components, (ii) Fabrication and assembly of the different parts and sub-assemblies, (iii) Flaw sizing and software activities to further refine detection and measurement capabilities, (iv) In-house testing of the integrated tool, and (v) System testing on the field. The activities under this contract are largely engineering in nature. This report is broken into the five areas listed above. Although there is significant overlap, the activities are largely chronological.

It is important to note that the actual EMAT/CRACK tool design went beyond what would have been necessary under this program. Although there are commercialization opportunities for a wireline tool, the larger market is for free-swimming tools. So, where practical, we implemented designs to support the longer-term goal of a free-swimming tool that operates at 2 m/s, navigates 1.5 diameter bends, and can be pressurized (2200 psi). The resulting tool configuration consists of two sensor modules placed in between three battery modules. As a result of the longer-term goal, it took a longer time for both the mechanical design and for the tool firmware development.

The pulser and receiver electronics of the EMAT/CRACK tool were revised, fabricated and tested, including new firmware. The communication board was also updated including additional processing power and an interface for gigabit ethernet for higher speed data transfers. The sensor module provides excellent signal to noise ratios, as much as a 16 times improvement over the Phase 2 tool. Rechargeable batteries were selected and installed on dedicated battery modules. The mechanical design of the tool was hardened as much as possible to survive the designed pressure and pipeline environment. Furthermore, a Graphic User Interface (GUI) for visualization of large data sets was coded. During this contract, our commercialization partner Q-Inline provided continuous support. The work packages included mechanical design of the modules, two rounds of testing at their pull-test facility in Texas, mechanical support preparing the setups and hosting the Qi2 team at their facilities, and lesser amounts of firmware and electronics.

After in-house and preliminary mechanical field testing, mechanical design refinements were included on the tool. Field testing of the EMAT/CRACK was performed at Q-Inline testing facilities in Texas on 8" diameter pipes with Schedule 20 and 40. The tool was able to navigate different types of bends (1.5-diameter and 3-diameter at 45^{o}) and diameter changes (i.e. insertion sections from 10" to 8") easily. Critical components such as wear pads performed well during tool cruising and exhibit increased survivability. In parallel, the tool was capable to gather data and inspect the pipes for manufactured cracks. All measurements were stored on the on-board memory and the systems was powered successfully by batteries. The data was downloaded and analyzed in a laptop. It was found that the tool was able to find not only cracks but also wall loss flaws during testing. Finally, this field test completed the successful development of the EMAT/CRACK wire tool. The next step on this program is the technology maturation for the free-swimming system.

2. SYSTEM DESIGN

On this section, the EMAT/CRACK wireline tool requirements were compiled and used to design the system. A discussion of the main mechanical and electrical features of the tool as well as some trade-offs are presented. Tool navigability was assessed using CAD simulations and parts fitting was checked with 3D printed components. These items are discussed on the following paragraphs.

Tool Architecture Design

At the beginning of this projected, a set of requirements were compiled to guide the EMAT/CRACK design on Phase 3 (Table 1). This information was used to enhance the proven Phase 2 tool architecture where a single sensor module was pulled through a 20' pipe length using a winch. An umbilical was used to provide power and download the data to a PC.

Based on the gathered data and architecture, a conceptual design for the EMAT/CRACK tool was developed and it is illustrated in Figure 1. Under this concept, instead of having a single module which received power and downloaded data via an umbilical, the tool had multiple pairs of modules. Each pair consisted of a battery module and a sensor module. Battery modules were placed and connected on the leading and trailing ends in order to provide physical support for the sensor modules for best centering.

Variable	Value	Comments
Pull Length	2 miles	Much longer for free-swimming
Pull Speed	0.5 m/s	2 m/s for free-swimming
Pull Modes	Calibrate, Run, Pause	Do not want the battery to die if paused for extended period of time
Battery Type	Li-Ion	Air shipping is not required for the wireline tool; per manufacturer Li-Ion is currently ok for Air Cargo (but not for passenger aircraft)
Shielding	Magnetic shield required	Based on air shipment restrictions
Battery run time	2 hours	For free-swimming tool, add capacity
Verification time	24 hours for full processing	Technician needs to know that data was good
Control Computer	Laptop	
Communication	Data will be read out from each module individually	
Calibration	TBD	When to perform calibration procedure
Onboard Processing	Not initially	Initially will store raw data and process on PC. Eventually process in real-time.
Wear pads	2 miles	
Battery removal	Optional	Battery modules may be swappable
Batt. Centralized	Required	Support the sensor module on the ends.
Bend	1.5D	Not required for wireline but adopting this requirement now will prevent redesign later.

Table 1. EMAT CRACK System Requirements.

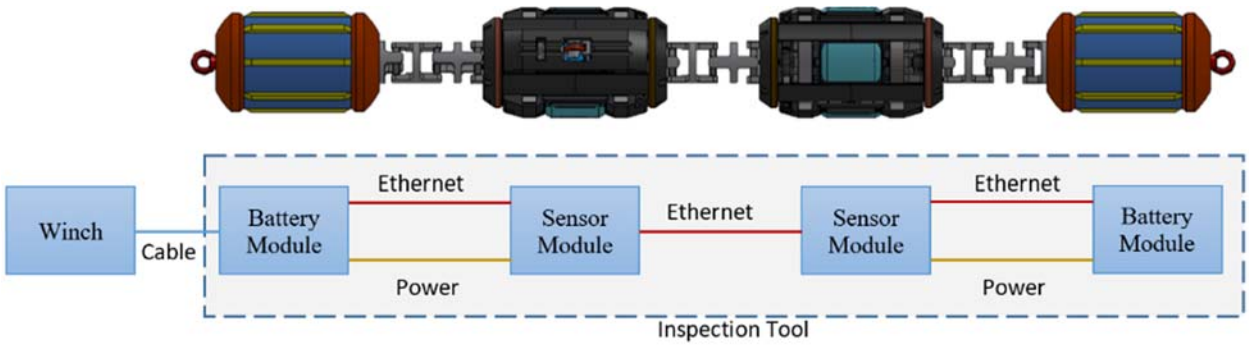

Figure 1. Conceptual Design of EMAT/CRACK System (Phase 3).

An Ethernet link run along the tool for communication. This link included both data and an encoder bus consisting of 4 pairs of wires. The end-end Ethernet link performed two main functions:

- Bi-directional communication between modules. This allowed features such as redundant use of encoders, so that in the event of the failure of a single encoder, the modules could share data from one that is working.
- Data downloading from one end. This allowed a technician to configure the tool and observe operation after it has been inserted into the pipe but before the scan has begun.

The new functionalities on the system required a number of changes which are illustrated in Figure 2. This initial architecture did not include a shared power bus. This means that individual modules had to be powered on or off at different times. The system software was in charge to be able to handle that situation.

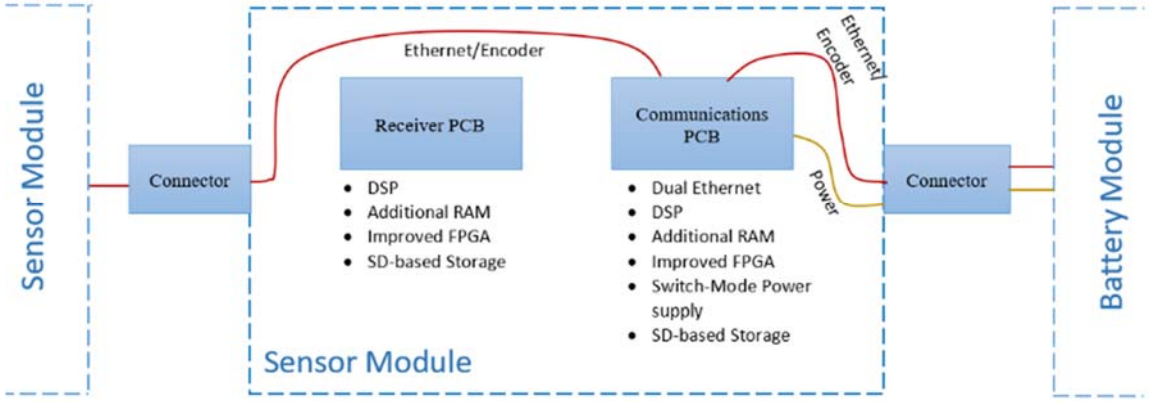

Figure 2. Sensor Module Enhancements.

Electrical Design Considerations

Pulser

The Phase 2 pulser design was revised in association with the EMAT Wall Loss program, and this revision was designed to be compatible with the requirements of guided-wave-based crack detection and sizing (i.e. 1/10th of the frequency). The lower frequencies mean that the waveforms were longer in time and therefore the total amount of energy transmitted per ping was greater. Therefore, the size of the pulser's

capacitor bank had to be large enough to allow the transmission of a pulse without excessive distortion. Some issues were found with the initial version of the new pulser, and these issues were resolved with a corrected board layout. The pulser design was fabricated and tested at both lower and higher frequencies.

The revisions implemented have substantially reduced the pulser's main-bang (i.e. initial pulse) recovery time and increased the power output. Although the crack tool operates on different principles than a wall-loss tool, main-bang recovery time was still important. This version of the pulser has higher current capability as compared to the pulser currently utilized in the Phase 2 crack tool. This provided stronger signals.

Receiver

In addition to the pulser, the receiver design was also revised. The receiver now incorporates much greater processing power, memory, a new analog front-end IC, and a low-noise amplifier with higher gain. These improvements further increased processing power and data throughput.

Communications Board (Comm Board)

The communications board (Comm board) from Phase 2 was revised to improve throughput (via gigabit Ethernet), increase processing power (with a DSP, RAM, and a more powerful FPGA), and provide for storage using an SD Card.

Battery PCB

The new system incorporated a battery module. In general, the batteries produce an unregulated voltage which must be converted into the 15V and 6V levels utilized by the EMAT electronics using a switched-mode power supply (SMPS). An SMPS provides a very efficient means of converting one input voltage into another, but it can be problematic for systems which are very sensitive to noise because of the transients generated by the switching. However, we identified a commercial part which was able to minimize the amount of noise generated. This was done by controlling the edge-transition rates and by utilizing a push-pull mode which has current flowing continuously except for brief transients which are easily filtered.

The broadband nature of the SMPS system, combined with the need to detect signals measured in microvolts, highlighted electrical noise level as an important design consideration. We spent considerable time analyzing the operation of the selected SMPS. It was found that the element of the design requiring the most analysis was the output transformer. We ended up designing and fabricating a custom transformer.

Besides power conversion, the Battery Module PCB also handles the encoder interface. To track the tool displacement along a pipe, two instrumented wheels were mounted on the sides of the sensor module, 180 degrees apart. One of the wheels (in red) can be observed on the first sensor module (left one) in Figure 1. Each wheel has a magnetic encoder to produce a pair of quadrature encoder signals which can be used to determine how far the tool has moved and in what direction. The two-wheel approach provides redundancy if one encoder slips, which can happen when going around bends, over a tee, etc., or if the encoder wheel becomes jammed with debris. In general, magnetic encoders are more robust than optical encoders in the presence of debris.

Battery Pack/Battery Management System

Our commercialization partner for EMAT/CRACK technology is Q-Inline, a company which has extensive experience fielding Magnetic Flux Leakage (MFL) tools. Although the sensor technology is quite different from EMAT, many of the system design issues are similar. We worked with Q-Inline to develop the battery pack which forms the basis for on-board power storage. The number and configuration of battery cells

was determined in consultation with Q-Inline. In addition, they selected the battery pack integrator to package and purchase the cells with the appropriate Battery Management System (BMS).

Mechanical Design Considerations

Tool Hardening

It is important to note that the Phase 3 project goal, as funded, was to improve the tool such that it could be used for wireline applications at 1 atmosphere of pressure. The primary objective at this stage of implementation was to expose the tool sensors and processing algorithms to a more diverse set of crack and other anomalies as well as potentially perform revenue generating work. So, replacement of wear components between deployments would be acceptable. However, the ultimate larger market is for the tool to be free-swimming, operate under pressure, longer distances, and faster speeds. Of course, none of these additional features were incompatible with a wireline deployment. Therefore, additional general tasks were included as follows:

1. Improvement of wear surfaces. Thanks to the cooperation work with Q-Inline, it granted us access not only to its MFL tool designs but also to its senior mechanical engineer to further improvement the tool wear and robustness.
2. Overall module design for extended use. Particularly, mechanical connections between the sensor sleds, carriers, and tool body.
3. Operating under pressure.
4. Differential pressure locomotion. This feature required seals to be designed to ensure locomotion and could set the minimum operating pressure and could impact bidirectionality. In addition, this activity required significant testing.

These additional longer-term tool hardening activities were performed under separate funding and were incorporated as they fit within the current project schedule and goals. Nevertheless, the Task 4 work was not performed since it was beyond the scope for this Phase 3.

Preliminary Wear Testing

On wear, a test fixture was designed and fabricated to test various materials. The materials selected for evaluation were Nylatron (Moly filled Nylon), UHMW and TIVAR (Special Type of UHMW). TIVAR was the material originally selected and tested during Phase 1 of this project.

Each material was tested until it failed. Failure was defined by any breach in the test sample pressure area. Operating at approximately 1m/sec (3.23 ft/sec) the distance was determined by the duration of the run. Two samples of TIVAR 0.030” thick ran for 5.59 and 5.22 miles. Three samples of UHMW 0.030” thick ran for 10.44, 22.37 and 26.9 miles. Test results determined that UHMW was the best material to use on wear surfaces with TIVAR being the second choice. Based on this we proceeded with prototyping all wear surfaces using these two materials. Metallic or Ceramic wear surfaces were not considered initially due to their long lead times between design iterations and cost. The UHMW material was found to be enough for the goals of the project at the time.

Operation at Pressure

Regarding tool operation pressure, we evaluated the conceptual electronics enclosure design and was found that its structure, if sealed, could not withstand an external pressure of 2.2kpsi. To produce an enclosure capable of operating at this pressure, the geometry, wall thickness and material of the enclosure had to be modified.

Detailed Mechanical Hardware Design

Based on the extended tool requirements and preliminary assessment, the EMAT/CRACK wireline conceptual design was reviewed, refined, and simplified in some important ways. At this point, the mechanical detail design work was transitioned to Q-Inline thanks to their expertise designing rugged MFL tools. It is important to note that during this process the electronics package was able to fit within the inspection module (EMAT Sensors). Furthermore, the electronics were now placed inside a pressure vessel that allows the system to transition to a free-swimming version easier on the next project phase. Figures 3 and 4 illustrate a five-module EMAT tool configuration using three battery modules and two sensor modules. The total length of this tool assembly is 76.375” with an estimated weight of 196Lbs. A close-up view of the U-link between modules is depicted in Figure 5.

Figure 3. EMAT Tool Assembly Modules

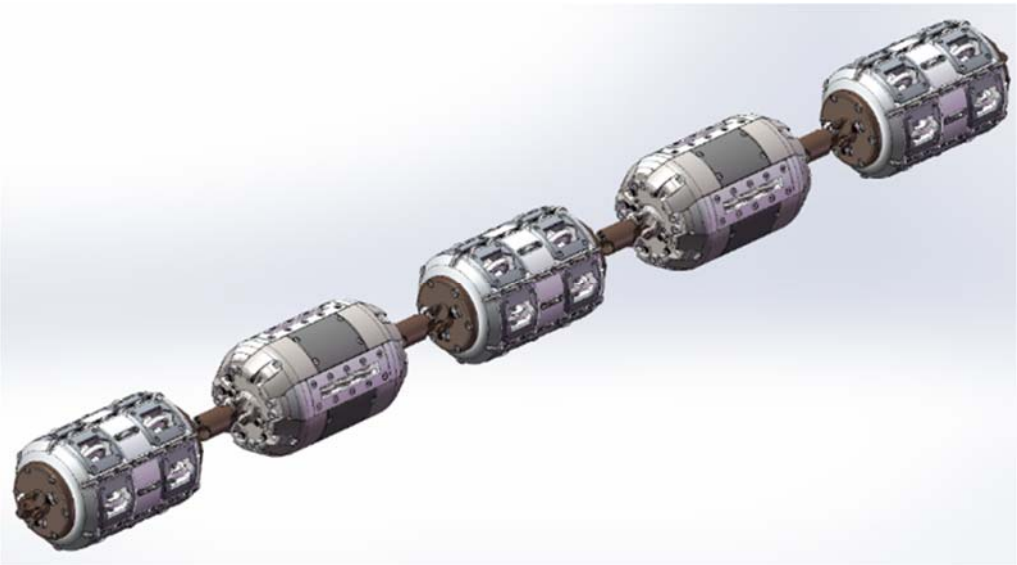

Figure 4. Perspective View of the EMAT Tool Assembly

The battery bus runs along the length of the tool. If additional battery capacity is needed for longer runs, more battery modules can be attached. Battery modules are attached in parallel (diode-coupled wired-OR configuration). The encoder wheels are now localized at the sides of the Battery Module. Likewise, the

odometer bus will run the length of the tool. One pre-determined battery module has its encoders enabled. The Battery Module PCB takes the raw signals from each encoder and combine them on one useful measurement.

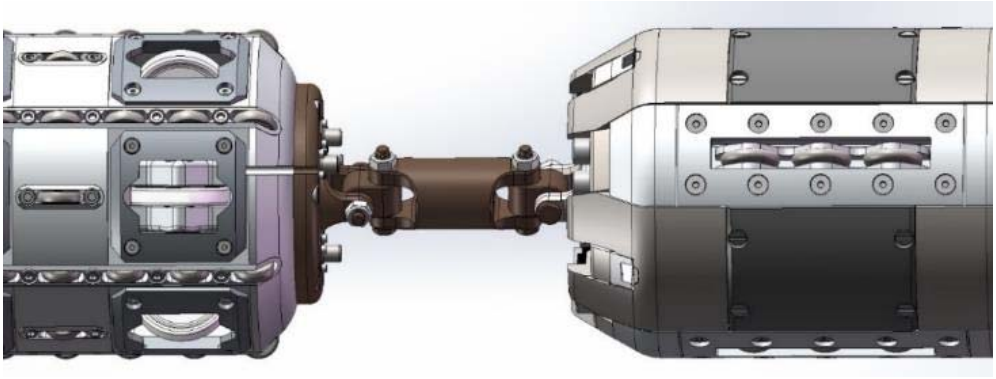

Figure 5. Detail View of U-Links Between Battery and Sensor Modules

The tool has been designed to navigate 1.5D bends on 8” diameter schedule 80 pipes. The Schedule 80 is the most critical thickness since it presents the smallest ID. The original requirements specified a maximum wall thickness of 0.5” (schedule 80). The design was verified by performing a CAD geometrical simulation (SolidWorks) through the bend where its main dimensions are shown in Figure 6. Some positions of the tool passing through the bend are illustrated in Figure 7. Here, the tool arrives at the bend (1). Next, the first EMAT modules passes the bend (2) followed by the second battery module (3). The second sensor module passes the bend (4) and finally, the tool leaves the bend (5).

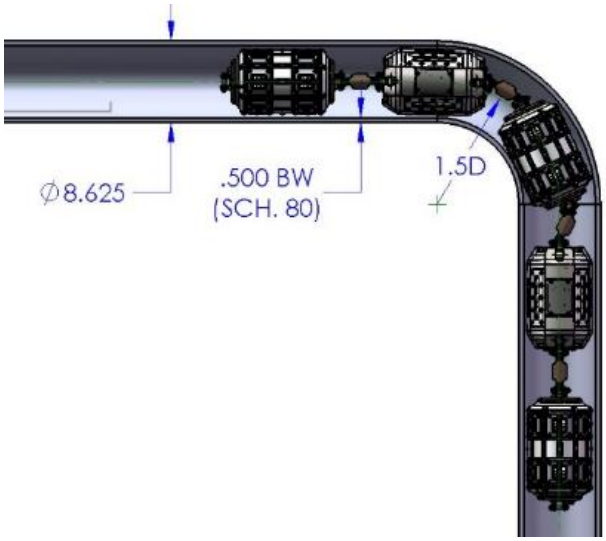

Figure 6. Dimensions of a 1.5D 8” Pipe Bend.

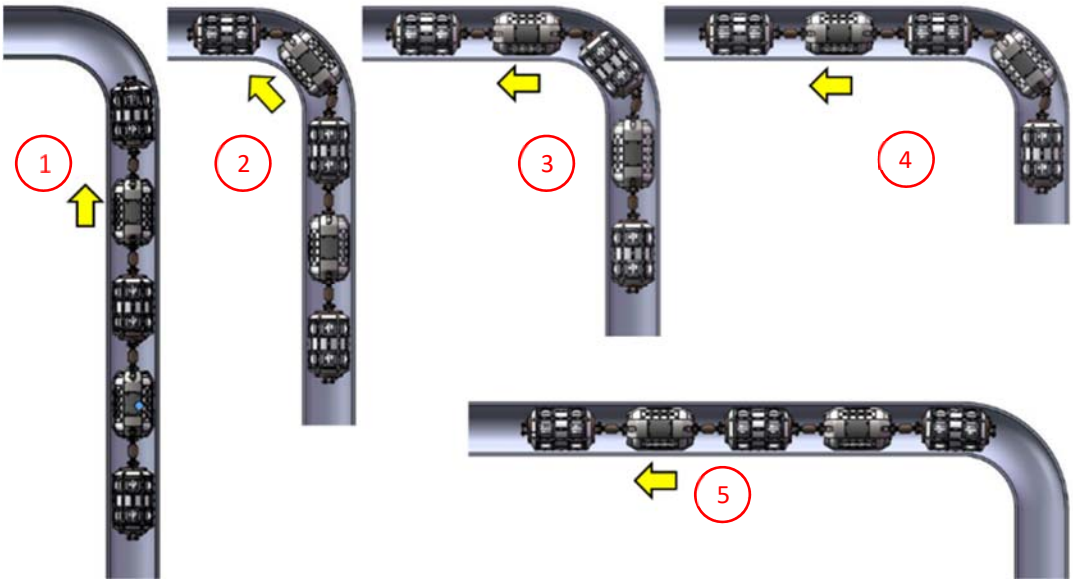

Figure 7. EMAT Crack Tool Passing Through a 1.5D 8" Diameter Pipe: Approaching (1), Passing (2-4), and Leaving (5) the Bend Section.

The *Sensor Module* can accommodate up to four EMAT sensors as well as their associated electronics inside a pressure vessel. The complete module is shown in Figure 8. The Sensor module was designed with a minimum diameter of 6.9" (retracted position) and a maximum of 8.63" diameter when extended as illustrated in Figure 9. The module has 12 connectors in the front bulkhead for connecting the EMAT sensors to the EMAT electronics and to the forward Battery module. There are two connectors in the module back bulkhead for communication with the backward Battery module. The estimated weight of the module is 39 lbs with a length of 11.625".

Figure 8. EMAT Sensor Module

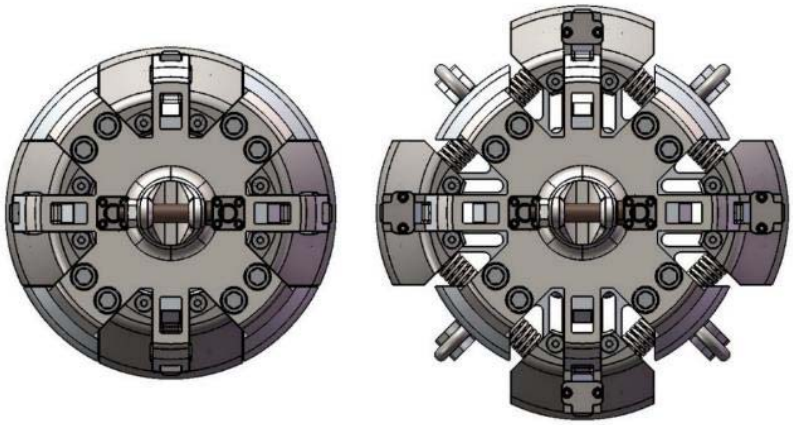

Figure 9. Front View of EMAT Sensor Module: Retracted (left) and Extended (Right).

One important feature of this design is that the pulser/receiver and communication board can be placed inside of a pressurized vessel. In the case of free-swimming ILI tools that are specified up to 150 Bar (2200 PSI), the pressure vessel safety becomes paramount. The pressure vessel has a one-way pressure release valve and a purge/vent plug as part of the end cap assembly. In addition, the purge bolt allows for vacuum testing the integrity of the module during tool commissioning and actually Nitrogen purging the inside of the vessel. Hence, it is operating in an inert atmosphere and this helps to reduce condensation by not having any air/moisture in the vessel.

After evaluating the EMAT tool main features, a 3D printed mockup of the sensor module was fabricated in ABS to verify fitting, assembly, cabling access, and cable service loops among other geometrical features. Figure 10 shows some views of the printed module in extended configuration. After the successful printing of the module, we proceeded with the actual tool fabrication and assembly.

Regarding the *Battery Module*, it is important to know what the power requirements of the system were key to size it properly. For a wire-line scan, the maximum distance was estimated to be 2 miles. At the planned speed of 0.5 m/s, this distance could take approximately 1 hour and 47 minutes to complete, ignoring any stops. This time, plus margin, determined the minimum run time for the system.

Figure 10. 3D printed EMAT Sensor Module. Top View (left) and Isometric View (right).

Based on a nominal runtime of 2 hours at 44 Watts, the minimum required battery capacity would be 88 WH, which can be met by a pack containing 9.2 cells.

Besides batteries, the battery module incorporated the following items:

- BMS: This is a PCB which provides safety protection for the battery pack against over voltage, over current, under voltage, over temperature, etc.
- Power regulator PCB. This PCB (described above) converts the raw battery voltage into the regulated 15V and 6V rails needed by the receiver and pulser. This PCB also takes the two-wheel encoders and merges them into a single output for use by the rest of the system.
- Wheel encoders. These provide a measurement of distance travelled.

Starting with a module that is as large as possible but can still negotiate a 1.5D bend, and reserving space for the above 3 components, the remaining space accommodated a pack containing 18 cells, which should support continuous operation for just under 4 hours. The cells were configured as two parallel strings of 9 cells each, for a nominal voltage of 32.4V. Figure 11 shows the Battery module. The total weight of the module is 38 Lbs with a length of 12.375”.

Figure 11. Battery Module: Front side (left) and back side (right)

3. FABRICATION AND ASSEMBLY

After the EMAT/CRACK tool architecture was optimized and the detailed design completed, the fabrication and assembly activities were performed. Mechanical components were machined, electrical PCBs were assembled and the whole system was integrated. Along this process, functional and geometrical checks were performed. These activities are discussed on the following sections.

Mechanical Subsystem

Once the detail design of the EMAT/CRACK tool were completed, components for the sensor carrier subassembly, including EMAT coils, were fabricated. At this stage, we used 3d printed components to verify fit. The sensor carrier subassembly was then mounted on a 3D printed Sensor Module quadrant to ensure proper installation, dimensions, and mechanical functionality. This fit check is shown in Figure 12.

Figure 12. Fit Check of the Sensor Carrier Subassembly with the 3D Printed Sensor Module Housing

The Sensor Module fabrication and assembly was coordinated by Q-Inline. The Sensor Carrier subassemblies were sent to Q-Inline for final integration. Two Sensor Modules were manufactured, and one is shown in Figure 13.

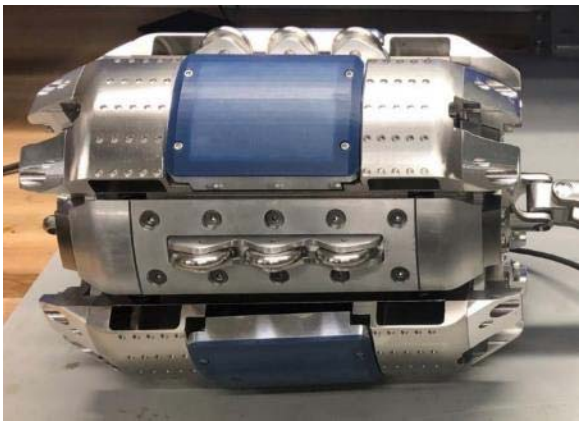

Figure 13. EMAT Sensor Module

Similar to the Sensor Module, the Battery Module fabrication and assembly was performed by Q-Inline. In total, two modules were manufactured and one of them is shown in Figure 14. The completed tool, including two Sensor Modules and two Battery Modules, is shown in Figure 15.

Figure 14. Battery Module

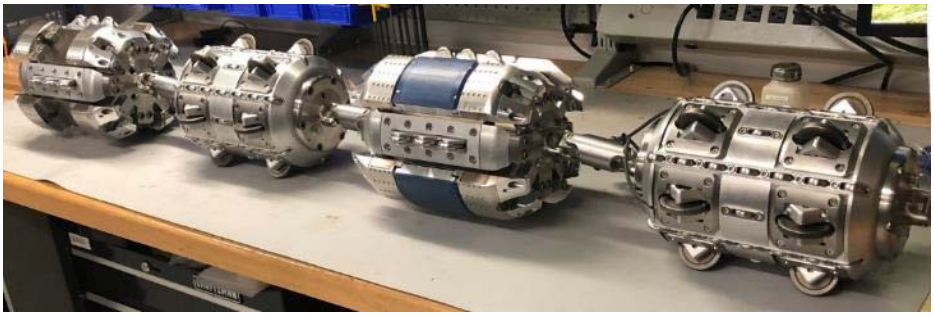

Figure 15. EMAT/CRACK Tool Modules

Electronical Subsystem

The pulser PCBs were fabricated (Figure 16-A) and tested at a wide range of frequencies. As discussed in the proposal, the Phase 2 pulser design was revised in association with a parallel project (EMAT Wall Loss program), and this revision was designed to be compatible with the requirements of guided-wave-based crack detection and sizing (i.e. 10x lower frequency). The revised receiver design was fabricated, and it is shown in Figure 16-B. The receiver now incorporates much greater processing power, memory, a new analog front-end IC, and a low-noise amplifier with higher gain.

Figure 16. Pulser PCB (A) and Receiver PCB (B)

The Communication PCBs (Comm Boards) were fabricated and two are shown in Figure 17. This board design was revised to improve throughput (via gigabit Ethernet), to increase processing power (with a DSP, RAM, and a more powerful FPGA), and to provide for storage using an SD Card.

Figure 17. Communication PCB

Li-Ion battery packs for the Battery modules were designed in two configurations: 9-cell and 18-cell. The 9-cell pack is shorter than the 18-cell pack. The 9-cell pack allowed the placement of encoder and power supply electronics inside that Battery Module. Each battery pack comes with its respective BMS board.

In order to provide regulated 6V and 15V from the batteries to the EMAT electronic components, a power supply PCB was designed and fabricated. A view of the assembled Power Supply is shown in Figure 18-A. This unit was installed at the end of the 9-cell battery pack. One PCB was configured for 15 volts and the other provides 6 volts. Because of the power levels and small package, the housing was designed to provide a heat path from key components on the power supply PCB's to the tool enclosure.

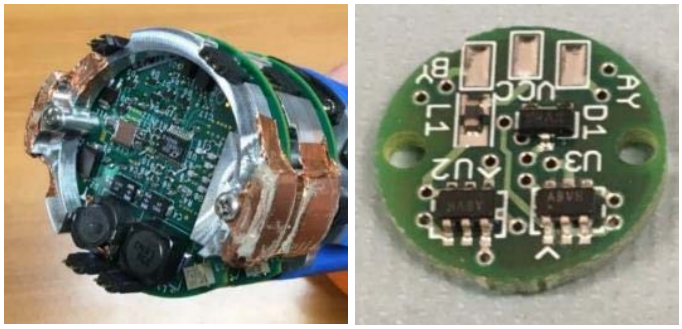

Figure 18. 15 Volt and 6 Volt Power Supply Boards (A) and Encoder PCBs (B)

Three encoder wheels were mounted on the battery module with the 18-cell battery pack, 120 degrees apart. Each wheel produces an encoder signal which is used to determine how far the tool has moved. Three encoders were used to provide redundancy in the event that one encoder slips, or if an encoder wheel becomes jammed with debris. The signals are gathered and processed by the Encoder PCB (Figure 18-B) mounted next to the Power Supply on the 9-cell battery pack module.

The sensor electronics PCBs were assembled and mounted on a monolithic electrical frame (E-Cage). The E-Cage provides mechanical, electrical, and thermal interfaces with the Sensor Module housing. The assembled E-Cage consists of two pulsers, two receivers, and the Comm PCBs. The final assembly within the Sensor Module is shown in Figure 19.

Figure 19. Installation of E-Cage on a Sensor Module

The Power Supply and Odometer PCBs were mounted on a 3D printed battery pack mockup to verify proper assembly. A fit check of the monolithic battery pack and PCB assembly was performed using a 3D printed Battery Module mockup. This fit check can be observed in Figure 20.

Figure 20. Power Supply Fit Check on a Battery Module Housing Mockup

Wiring and Battery System

The wiring and installation of the electronics into the sensor module was completed (Figure 21). The batteries and power supplies were wired and integrated in the Battery Module. This module was tested successfully. It is important to note that wiring turned out to be more tedious than originally thought due to small connector sizes and required cable sizes and flexibility. We will eventually need to order custom cables for the free-swimming version of the tool. Also, the connectors used are not pressure compatible mostly due to long lead times for high-pressure ones. The assembled tool is shown in Figure 22.

Figure 21. Sensor Module

Figure 22. Assembled and Connected EMAT/CRACK Tool

Firmware

Critical to system operation is the firmware which resides on programmable parts. On each receiver and communication board are two programmable parts, a Field-Programmable-Gate-Array (FPGA) and a Digital Signal Processor (DSP). The FPGA performs processing tasks which must occur in parallel at high speed, such as receiving digitized sensor data from the Analog to Digital Converter (ADC, sometimes referred to as the AFE). The DSP performs higher-level, more complex functions such as filtering and packetization. In the future additional processing tasks will be added to support the free-swimming tool.

The primary firmware-related tasks for this Phase 3 project involved implementing an architecture (Figure 23) which would:

- Support a faster ping rate up from 104 Hz in the previous system.
- Work for our wall-loss EMAT system as well as the crack tool. Utilizing a common code base means that any features implemented for one tool could also benefit another, at little or no additional cost.
- Support the incorporation of additional onboard processing, something that will be critical for reducing the volume of data produced by a free-swimming tool.

The basic tasks for the receiver involved acquiring sensor data from the ADC, filtering it (i.e. vertical processing), and transmitting it upstream to the communication board. Data comes from the ADC in two serial channels at very high speed. This data is buffered into several pings and transferred to the DSP at one time.

Formerly each ping was transferred to the DSP separately, but this makes for a very complex software architecture as all operations had to be broken up into small, interleaved sub-tasks. Transferring several pings at once allows the DSP to filter all the data at one time, which is a much simpler operation. The larger amount of memory and dual data paths also allows the DSP to perform this filtering (or other processing) at the same time that new data is being acquired and transferred.

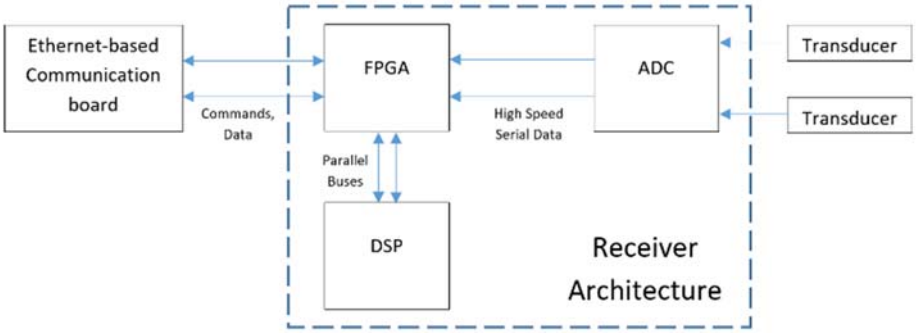

Figure 23. Improved System Architecture

Other firmware-related activities performed on this project included:

- Corrections to the FPGA code, especially relating to data transfer between the DSP and FPGA, and the DAC which is used to set the front-end gain.
- Optimizing system startup
- SD Card storage and Gigabit Ethernet on the Comm Board.
- Data downloading from the tool to a PC computer.
- Odometer firmware, which combines input from multiple encoders into a single stream.
- Increasing the speed of the data through electronics and firmware was constant ongoing process.

We also improved the communications protocol between the communications board and the PC. Although the wire-line tool stores all data onboard, for lab testing an umbilical was used to transmit the data in real-time to a PC. Improvements to this code provided a closed-loop confirmation that commanded setting changes took effect.

4. FLAW SIZING AND SOFTWARE ACTIVITIES

A constant activity performed along this Phase 3 was the refinement of the EMAT/CRACK detection and measurement capabilities as well as how to handle the information. A summary of this effort is presented on the following paragraphs.

Display Software

We recognized the fact that we may need to use two modules to improve redundancy. Therefore, we modified features of the GUI to include two displays. The software can load two data files. It can also automatically align the two displays based-on the flaw-signatures. Large datasets cannot be loaded in their entirety for processing because computers have finite memory. We now have implemented methods to read, process and display the dataset in manageable sections or parts. Several other small modifications to help in report writing were also included. These include allowing the displayed reports to pop-up into a stand-alone figure(s) that can be save saved at high-resolution; methods to change the contrast of the images and interfaces to exhibit raw data at a point of interest on the scan-image.

Improved Signal to Noise Ratio

More powerful magnets were incorporated into the EMAT design. As a result, the signal to noise ratio has greatly improved. This will lead to improved flaw-sizing accuracy. Improved signal to noise ratio also means less preprocessing of the signals. This in turn helps increase the rate at which the pipe can be scanned setting the stage for the free-swimming tool speed (2 m/s).

Flaw-Sizing Activities

In the previous Phase 2 of the project, 8” schedule 40 pipes with electro-discharge-machined (EDM) notches were used to test the tool and the ability to size crack-like flaws. It was anticipated that EDM notches would be the closest to cracks found in the field. However, we found that at least for the samples at hand, the EDM method was not very accurate. We therefore had difficulty in correlating the sizing results and the specified crack-sizes. To find out the actual depths, phased array ultrasonic testing (PAUT) operated by a technician (from an independent organization) was employed. However, PAUT itself has tolerance of +/- 1 mm – which is large when compared with the pipe wall thickness. Further, the technician reported undulating crack depths. Another method to produce real-life crack is to use a method involving thermal fatigue. According to the vendor, this method also has a tolerance of +/- 1 mm. Thus, it is very hard to manufacture flaws that resemble true cracks with good accuracy. Therefore, we machined notches of controlled depths using a fly-cutter and equipment available in-house. These pipe samples were scanned and sized using our sizing algorithm. Additionally, finite element analyses (FEA) of the wave propagation in pipes with notches were performed for the sake of comparison. Sizing results from the experiment data and FEA data were found to have good correlation. Finally, after calibrating the trends, there was good agreement between measurements and actual notch depths as shown in Figure 24. The legends corresponding to R1, R2, R3, R4 are relative orientations between the transceiver and notch as shown in Figure 25.

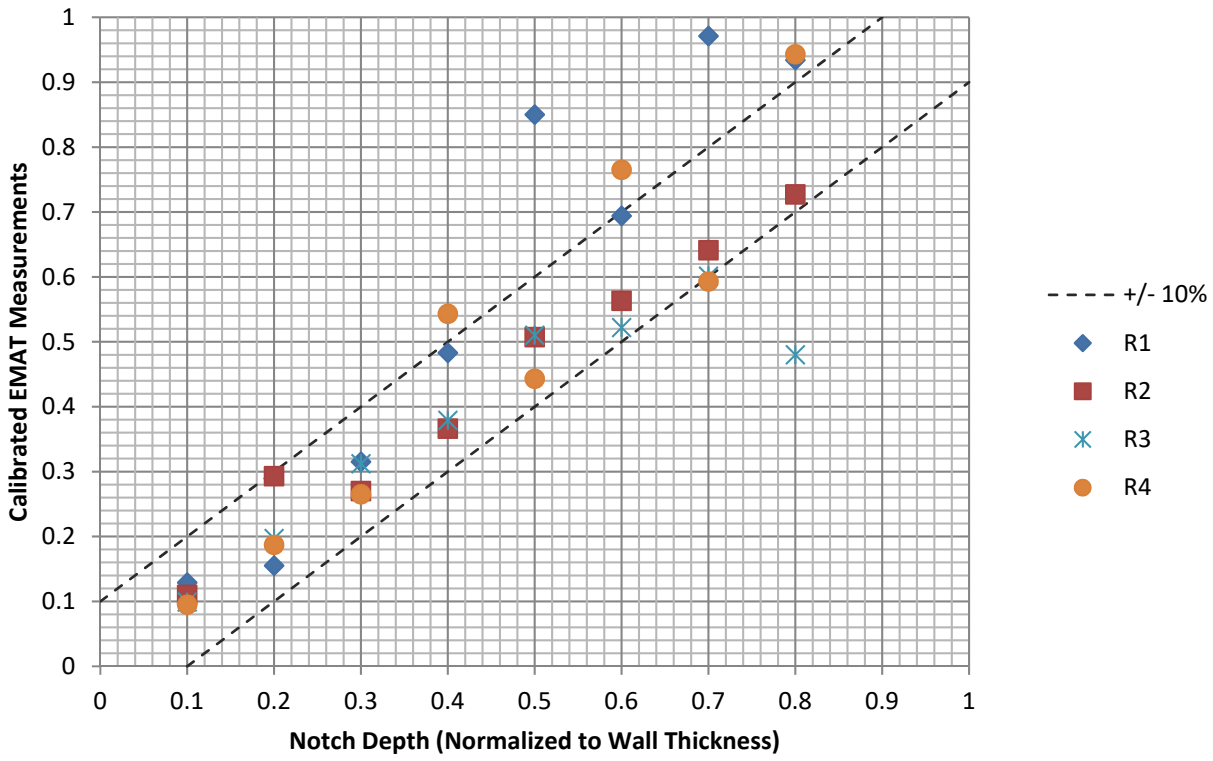

Figure 24. Calibrated EMAT measurements for fly-cutter notches in pipes. The legends R1 to R4 represent the various configurations between the receiver and notch as shown in Figure 25.

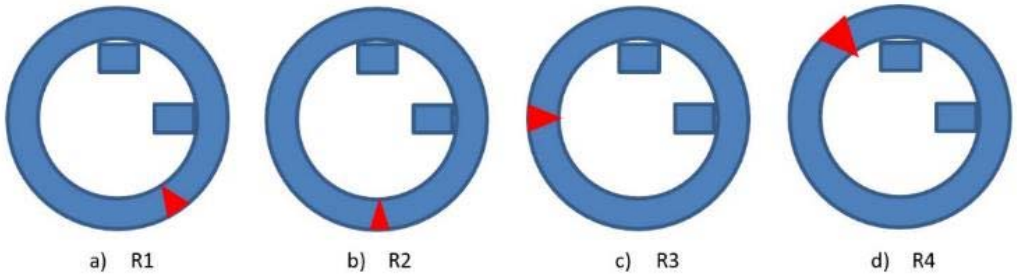

Figure 25. Tool orientations for Figure 24.

5. IN-HOUSE TESTING

After assembly the EMAT/CRACK modules and tool, the tool was tested at different levels: electrical, mechanical, and operational (i.e. flaw detection). These assessments were performed at Qi2 facilities. Key activities and results are reported on the following sections.

Mechanical Debugging

In order to test the mechanical tool capabilities in-house, we redesigned and updated our test fixture where two electrical winches are used to pull the EMAT/CRACK tool. The revised fixture is shown in Figure 26. Preliminary pull testing was performed at Qi2 where we found some mechanical interference issues between the tool housing and the mechanism for extension and retraction of the sensors. These items were addressed by re-machining some parts, redesigning of some components, and/or using different materials.

Figure 26. Revised Test Setup

Electrical/System Testing

A dynamic round of sensor testing was performed at Qi2 using the new pulser, receiver, and firmware with an ethernet cable connected to a computer. The setup and gathered signals are shown in Figures 27 and 28, respectively. An 8:1 improvement in signal to noise ratio was observed in the Phase 3 tool when compared with the Phase 2 version of the tool. If we consider the fact that the driving current for Phase 3 tool is half that of Phase 2 tool, the real improvement is likely to be 16:1. This figure was calculated by comparing the strength of the acoustic signal versus the electrical noise (see Figure 29). The calculations for this ignore the effect of winch noise.

As mentioned before, the tool is pulled by an electrical winch. The electrical signals fed into the motor seem to be wirelessly transmitted to the EMAT tool. Figure 30 shows a better way of comparing the effect of winch noise in the signals from Phase 2 and Phase 3 tools. The winch noise occurs randomly and when

several sets of signals are superimposed, their effect becomes apparent. Clearly, the improvement of signal to noise ratio in terms of winch noise in the Phase 3 tool is much better that it may be qualified as incalculable.

Figure 27. EMAT/CRACK Sensor Module (left), and Test Setup (right)

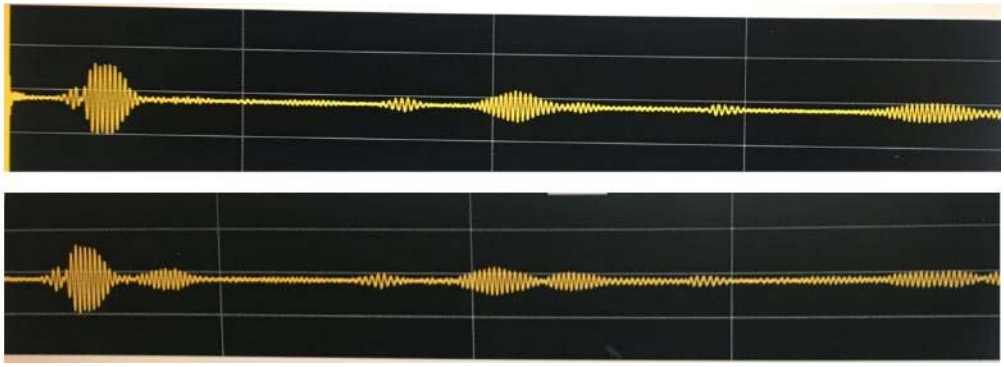

Figure 28. Gathered EMAT/CRACK Acoustic Responses for no-flaw (top) and flaw (bottom)

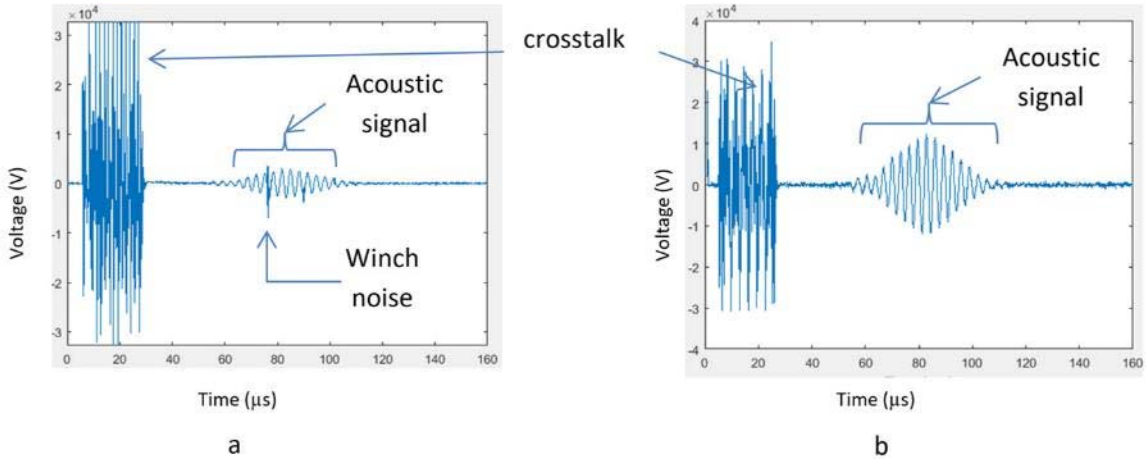

Figure 29. Comparison of signal strengths for a) Phase 2 tool and b) Phase 3 tool. This resulted in a 8:1 improvement in signal to noise ratio

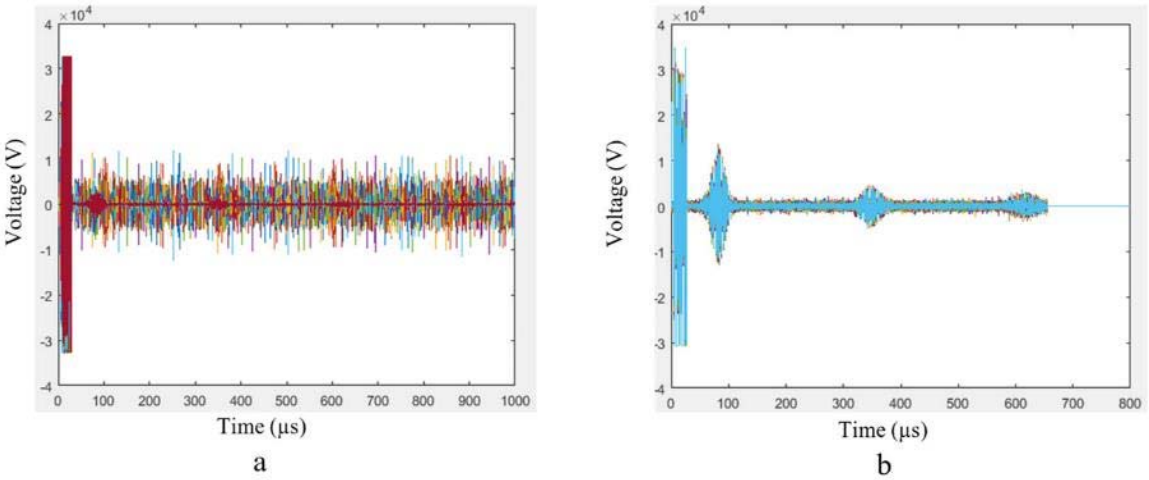

Figure 30. Comparison of winch noise for a) Phase 2 tool and b) Phase 3 tool. A set of 77 signals were superimposed for this illustration.

Once the EMAT/CRACK system was assembled, it was tested for functionality inside one of the pipes as shown in Figure 31. The tool operated with an 18-cell module. Data was transferred over an Ethernet cable into a computer. A screen shot of the acoustic responses from the first battery powered tool test is shown in Figure 32.

Figure 31. Assembled EMAT/CRACK System

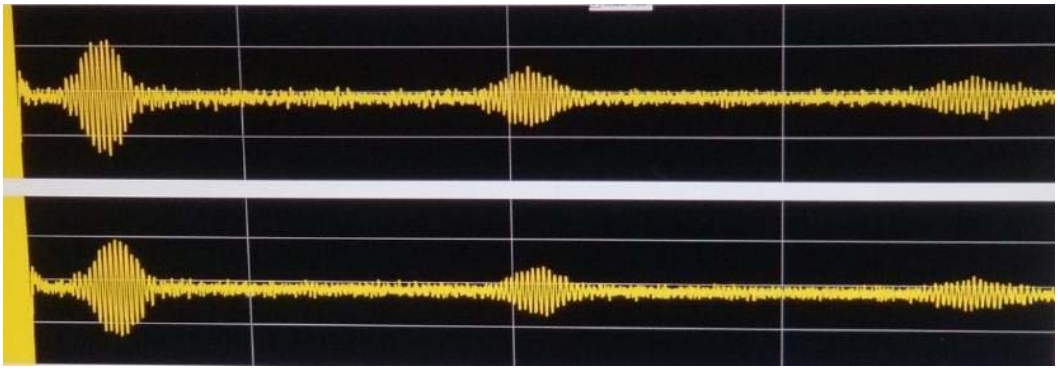

Figure 32. EMAT/CRACK System Responses

Final Electrical Integration

In parallel to the mechanical testing of the system, the sensor and battery modules were further integrated and tested. The tool was fully powered by the battery modules with all the data being recorded and stored locally on the tool. Encoder signals were also captured by the firmware and stored on the tool. Typical signals are shown in Figure 33.

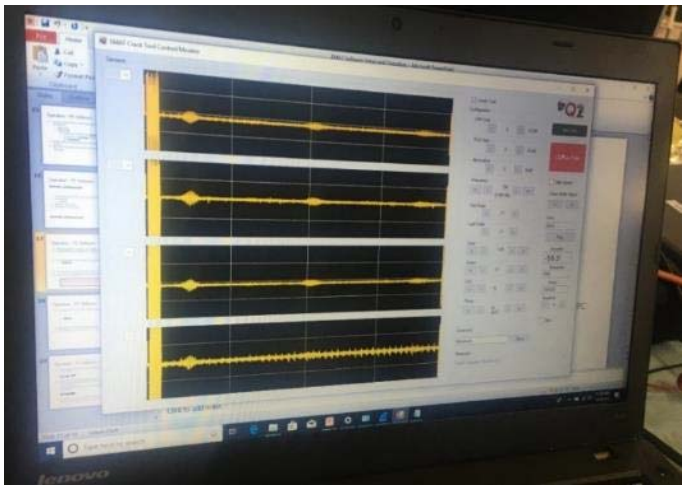

Figure 33. Signals from the Fully Integrated EMAT/CRACK Tool.

Flawtech Sample

We were often faced with the question if the EMAT Crack tool could detect tight cracks. Previously, only machined flaws were available for testing. We employed the services of Flawtech to create tight cracks using their thermal fatigue technique. An X-52 pipe with 8" OD and schedule 40 (no coating) was selected for this task. The length of the spool was 3' 8". A drawing of the Flawtech sample with two ID-side and two OD-side cracks of 2mm and 4mm depths for each side is shown in Figure 34.

To assess the EMAT CRACK performance, the tool was tested on the Flawtech sample to detect the fabricated cracks. Since, we were not able to visually identify the cracks, the Qi2's magneto-optic imager system (MOI^{TM}) was used to obtain an understanding of where exactly the cracks were located (See Figure 35). There was significant material removal on the pipe ID, perhaps to facilitate the cracks fabrication by thermal fatigue. As a result of this significant variation in wall thickness, sizing results using the crack tool data were unreliable. In addition, the crack depths are only certified to +/- 1 mm. Two of the flaws were intended to be 2 mm deep while the other flaws were intended to be 4 mm deep. The material removal is itself a flaw category (wall loss). Even with the inconsistent wall thickness, we were able to successfully detect three of the four cracks in the sample. We suspect that one of the 2 mm flaws were at the bottom of the tolerance allowance (1 mm). All these results are illustrated in Figure 36. The significance of this result is that it demonstrates the ability of the EMAT crack tool to detect tight/closed cracks which were not previously available to us. It is important to note that the x-axis values in Figure 36 do not represent true length of the pipe as encoder subsystem was not fully functional at the time of the test and the pulling speed of the in-house winches was not consistent over the short length of the sample.

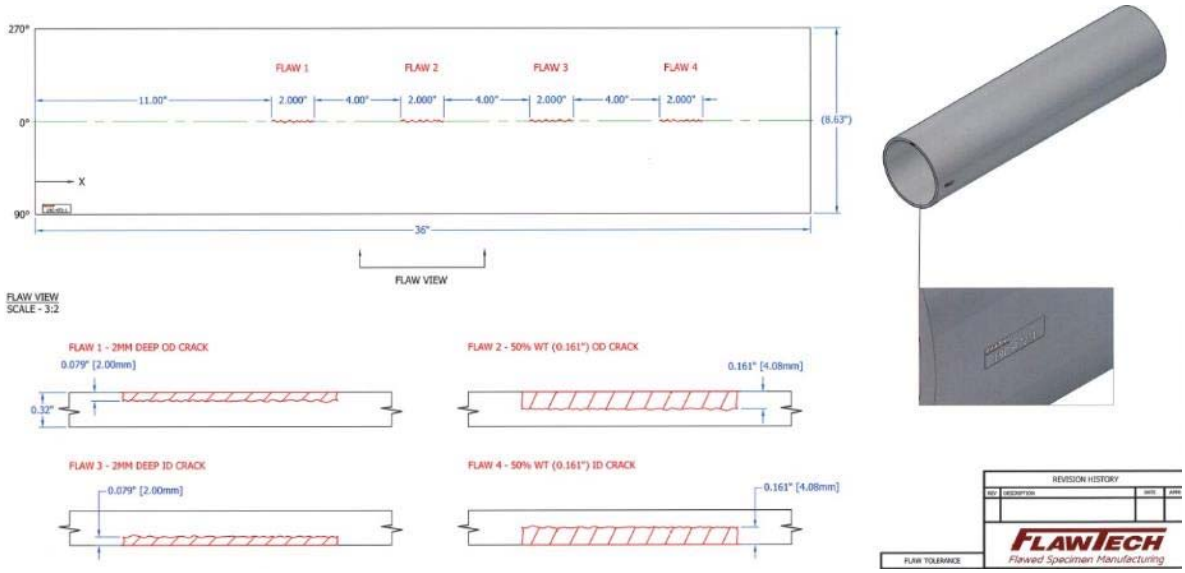

Figure 34. 8" Pipe with Cracks for Testing

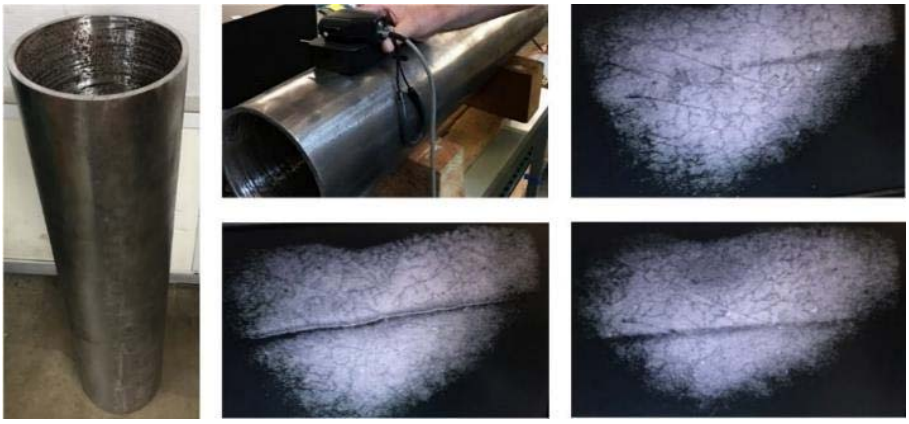

Figure 35. Flawtech Sample (left), MOI Setup (Top Center), and MOI Crack Responses (Center/Right).

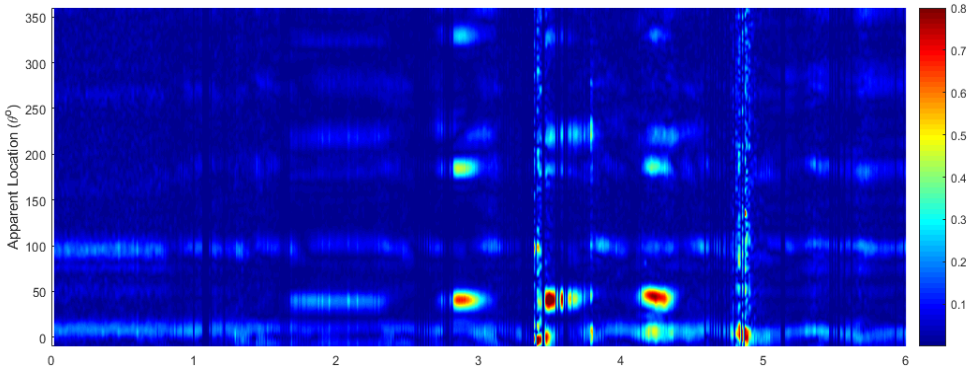

Figure 36. EMAT Crack Tool Responses. At Least Three of 4 Cracks are Identifiable both by MOI and EMAT Crack Tool.

6. SYSTEM FIELD TESTING

Field testing activities were performed gradually. First, the EMAT/CRACK system was divided in two parts: (i) One sensor module and battery module that was based at Qi2 for further electronics tuning and testing, and (ii) One sensor and battery module pair that was based at Q-Inline for field testing and mechanical modifications. Lessons learned from both testing fronts were integrated into systems for a final field testing at Q-Inline facilities in Texas. Main field-testing exercises and tool modifications are summarized on the sections below.

Mechanical Testing - First Iteration

A pull test was performed by Q-Inline at their testing facilities in Texas using one battery module and one sensor module (no signals were recorded). An 8" diameter and Sch 20 pipeline was used here and the setup is shown in Figure 37. The goal of this test was to assess mechanical performance during introduction, straight pipe movement (3 hrs. of continuous pulling) and bending navigation. The tool was pulled 50 times making 1 mile of travel distance. The general condition of the tools was mechanically sound with all mechanical parts still moving in and out without locking up, all wheels were rotating with no flat spots. However, the wear pads exhibited excessive wear and one of the universal links connecting the modules broke due to high stresses/loads during tool insertion (Figure 38). Pulling loads on straight pipe were found to be similar to those performed at Qi2 facilities (~580lbs). According to Q-Inline, these loads are almost 1/6th of the ones experienced by equivalent MFL tools. It is important to note that a lower pulling force means that the differential pressure needed to propel an EMAT free-swimming tool is also lower in comparison with those pressures required to run an equivalent MFL tool. This is a very key feature as low-pressure lines can make the line unpiggable by traditional MFL tool due to the large differential pressure requirement for proper flow.

It is important to note that we performed extensive in-house testing on the TIVAR wear pads. However, during the field test in Texas, the pipe temperature was high with an ambient temperature of greater than 90^{o}F and the pipe was under the sun. After the 1-mile pull test, the tool temperature was too hot to touch. We suspect that the tool temperature was greater than the maximum operating temperature of the TIVAR wear pads, degrading its performance. Unfortunately, the temperature of the pipe or the temperature of the tool after the test were not measured. In a real pipe, the line will be buried and out of the sun at significantly lower temperatures.

Figure 37. Tool Insertion and Loop Setup

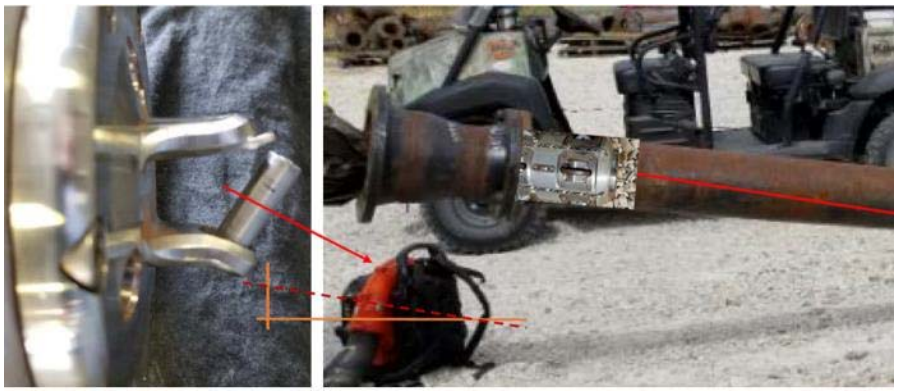

Figure 38. Broken Link during Insertion

Design Rework

Based on the in-house and field testing, we optimized the mechanical design of the tool. In particular, we redesigned the wear pads on the sensors and yoke shoes as well as the U-Joint links and endcaps. In the case of the sensor wear pads, one design was based on high temperature TIVAR and the other one on a ceramic based material. A fixture was designed to test those parts in-house and it is depicted in Figure 39. Here, a pipe section with a rough girth weld is used as a contact surface for the wear pad assessment.

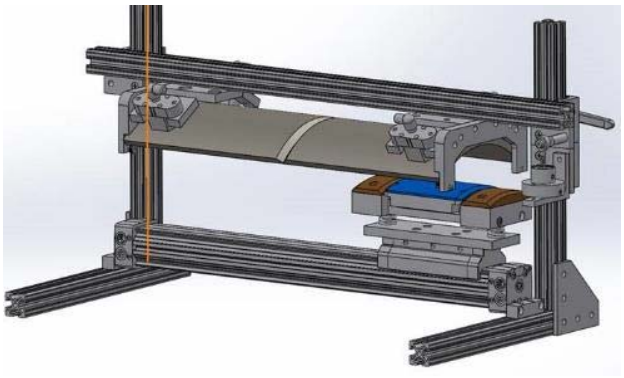

Figure 39. Wear Pad Fixture Setup

In the case of the high temperature TIVAR, the sample was run for 2.5 miles using aluminum oxide as an abrasive media. Some grooves were worn into the pads to a maximum depth of 0.01" in some spots. The pipe weld was worn down flat and the pipe wall itself sanded down to a shiny surface. These results were encouraging. Therefore, we retrofitted the system with these design for further field-testing. The ceramic design had long lead times. Therefore, only one iteration was possible to be assessed on this Phase 3 project. In any case, the ceramic pads would be used on the free-swimming version of the tool. It is important to note that we are looking at ways to reduce the friction and heat generation as a precaution.

After analyzing the failure of the U-joints during field testing, several components were redesigned and their materials, in some cases, were replaced by titanium. Finite element simulations were performed to compare the "failed" design (i.e. current), with a new design with 431SST and one with titanium. This design was 3D printed (Figure 40) to ensure 1.5 OD bending navigability and no interference between connectors and links. A view of the design during navigation testing is shown in Figure 41.

Figure 40. 3D Printed prototype for Link between Modules

Figure 41. Navigation Test for New Link Design

Mechanical Testing - Second Iteration

We traveled to Q-Inline testing facilities in La Grange, TX and performed a second iteration on mechanical testing. The goal of this session was to assess the new wear pad designs (TIVAR and metallic shoes) as well as new joints between modules. The tool was tested on a 100ft section of 8" diameter pipe (See Figure 42) using a 10" to 8" reducer to insert the tool (Figure 43). Two winches, one at each end of the pipe, were used to pull the tool in both directions. After a 200ft run (back and forward), it was found that two wear pads were damaged. The wear pads were replaced, and the tool was run for 1 mile. At the end of the run, the wear pads were found damaged again.